Highlighting manganese transport mechanisms in the nervous system with MEMRI in *Aplysia californica*

Ileana Ozana Jelescu[1], Romuald Nargeot[2], Denis Le Bihan[1], and Luisa Ciobanu[1]
[1]*NeuroSpin, CEA/DSV/I2BM, Gif sur Yvette, France,* [2]*Université Bordeaux 1, CNRS UMR 5287, Bordeaux, France*

Introduction *Aplysia californica* is a widespread model in neuroscience[1-3]. Its main advantages over mammalian systems are its large cells constituting networks of identified neurons, and the cells' tolerance to non-ideal conditions. In this manganese enhanced MRI (MEMRI) study, we explore the manganese (Mn^{2+}) transport mechanisms in resting state and following dopamine (DA)-induced neuronal activation, in the buccal ganglia of *Aplysia californica* (DA is a modulatory transmitter which activates the buccal neuronal network). Understanding the pathways of Mn^{2+} transport in the nervous system is of paramount importance as many recent studies[4,5] use Mn^{2+} as a neural tract tracer in mammals. Moreover, DA is involved in numerous physiological functions (motion, reward mechanisms, memory…). Our study can also lead to a better understanding of the dopaminergic modulation mechanisms in a motor network and the evolution of the latter with dopaminergic reward system.

Materials and methods In a first study, three *Aplysia* were anesthetized by injection of a $MgCl_2$ solution (360 mM). The bilateral buccal ganglia were resected and placed in artificial sea water (ASW). Each ganglia pair was used for unilateral Mn^{2+} migration along one motor nerve: nerve 2 (n.2), 3 (n.3) or esophageal (E.n.) (Fig. 1). The nerve at stake was isolated in a vaseline well and dipped in a solution of intracellular medium + $MnCl_2$ at 25 mM. After 18h at 4°C, the ganglia were inserted into a 1.5 mm diameter glass capillary filled with ASW. MR imaging was performed in a 17.2T magnet (Bruker BioSpin) using a home-built microcoil as RF transceiver. Imaging consisted of a 3D FLASH (TE = 2 ms / TR = 150 ms / 25µm isotropic / 2h40) for T_1 contrast and of a 3D RARE (TE_{Eff} = 18.4 ms / TR = 3 s / 25µm isotropic / 1h20) for T_2 contrast. T_1-weighted (T1w) images show regions of Mn^{2+} uptake (hyperintense) while T_2-weighted (T2w) ones show all cell bodies (hypointense). In a second study, the same Mn^{2+} migration protocol along n.3 was applied on a fourth animal. Prior to imaging, the ganglia were perfused for 2h with a solution of ASW + DA at 50 µM. The imaging protocol was unchanged. A fifth *Aplysia* was used for electrophysiological measurements to test whether the Mn^{2+} concentration used compromises the functionality of the neuronal network and the cells' viability. These measurements were performed after the same preparation protocol on n.3.

Results and discussion Images following Mn^{2+} migration along n.3 (without DA) are shown in Figure 2. Cross-comparison between T_1w and T_2w images allowed the identification of neurons loaded with Mn^{2+}. In this case, all enhanced neurons corresponded to cells with known axonal projections in ipsilateral n.3. The neurons enhanced by Mn^{2+} migration along n.2 and E.n. were also those with known axonal projections in each of these nerves (images not shown). The Mn^{2+} distribution in the ganglia following a 2h perfusion with DA appeared very different from that without DA (Fig.3). The directly loaded cells on the ipsilateral side were less hyperintense, while Mn^{2+} seemed to be present on the contralateral side into two cells with no direct axonal projection in ipsilateral n.3. This result supports the hypothesis of intercellular Mn^{2+} transport with neuronal activation. Simultaneous intracellular recordings of both B4 neurons (Mn^{2+} loaded and contralateral unloaded – see Fig. 1b) and extracellular recordings of the ganglia motor outputs showed that the functionality of the neuronal network was not impaired at this Mn^{2+} concentration.

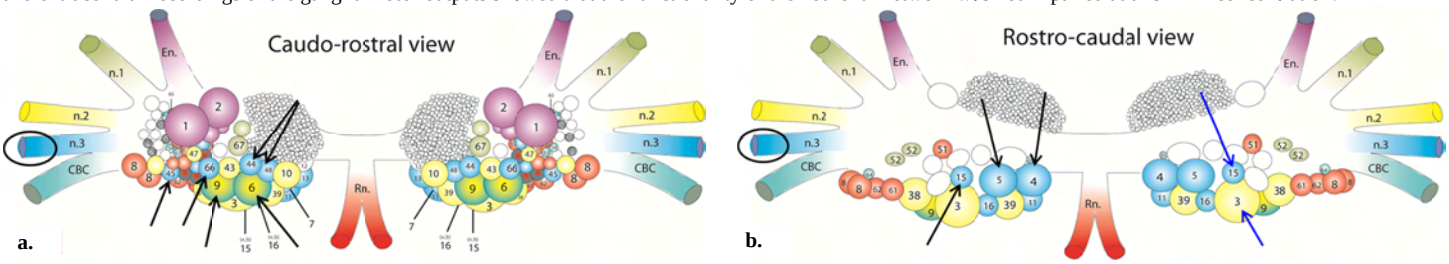

Figure 1. Schematic of nerve-neuron relationships in the buccal ganglia. In (a) the arrows point to cells labeled in Fig. 2b after Mn^{2+} migration along left n.3 (circled). In (b) the arrows point to cells labeled in Fig. 3b after Mn^{2+} migration along right n.3 (circled) and DA perfusion.

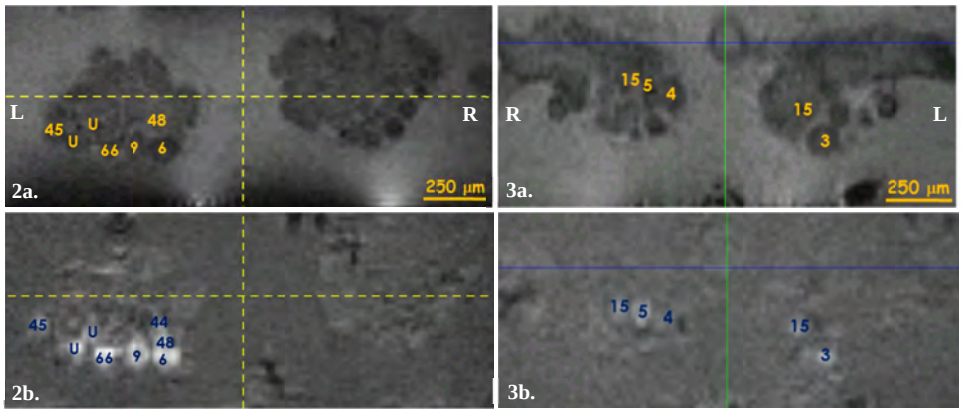

Figure 2. 17.2 T T_2w (a) and T_1w (b) representative images of the buccal ganglia following Mn^{2+} migration along left n.3. The hyperintense regions in (b) were identified as neurons with known axonal projections in ipsilateral n.3 (see Fig. 1a). Additional slices (not represented) showed the labeling of B4-5-11-15-16.

Figure 3. 17.2T T_2w (a) and T_1w (b) images of the buccal ganglia following Mn^{2+} migration along right n.3 followed by DA perfusion. The ipsilateral hyperintense cells in (b) were identical to those labeled in the absence of DA. The contralateral hyperintense regions were identified as neurons (B3 and B15) which have no axonal projections in right n.3 (see blue arrows in Fig. 1b).

Conclusion These results show, for the first time using MEMRI, the Mn^{2+} transport along known axonal projections and the DA-induced intercellular transfer of Mn^{2+} between identified neurons of the buccal ganglia of *Aplysia californica*. This DA-induced Mn^{2+} transfer in the buccal network is currently retested by pre-/post-DA imaging in the same pair of ganglia. The identification of the synapses through which Mn^{2+} is transported after DA addition will enable us to determine whether the synaptic Mn^{2+} transfer is electrical, chemical or both and/or whether an extra-synaptic diffusion is involved. This study may further shed light on the mechanisms of inter-neuronal communication within a DA-modulated motor network.

References [1] I. Kupfermann and E.R. Kandel, Science 164 (1969) [2] J.S. Schoeniger *et al*., JMR Series B 103 (1994) [3] R. Nargeot and J. Simmers, Cell Mol Life Sci. 68 (2011) [4] R.G. Pautler, A.C. Silva and A.P. Koretsky, MRM 40 (1998) [5] J.M. Simmons *et al*., J Neurosci 28 (2008).
Acknowledgments The authors acknowledge technical support from B. Djemaï and financial support through grant ANR-08-PCVI-0009-01.